FEBS Letters 584 (2010) 4009–4014

journal homepage: www.FEBSLetters.org

The double mutation ΔL6MW241F in PsbO, the photosystem II manganese stabilizing protein, yields insights into the evolution of its structure and function

Hana Popelkova [a,*], Alan Commet [a], Charles F. Yocum [a,b]

[a] Department of Molecular, Cellular and Developmental Biology, The University of Michigan, Ann Arbor, MI 48109, USA
[b] Department of Chemistry, The University of Michigan, Ann Arbor, MI 48109, USA

ARTICLE INFO

Article history:
Received 22 June 2010
Revised 27 July 2010
Accepted 8 August 2010
Available online 12 August 2010

Edited by Richard Cogdell

Keywords:
Evolution
Manganese-stabilizing protein
Mutation
Photosystem II
Thermostability

ABSTRACT

The W241F mutation in spinach manganese-stabilizing protein (PsbO) decreases binding to photosystem II (PSII); its thermostability is increased and reconstituted activity is lower [Wyman et al. (2008) Biochemistry 47, 6490–6498]. The results reported here show that W241F cannot adopt a normal solution structure and fails to reconstitute efficient Cl^- retention by PSII. An N-terminal truncation of W241F, producing the ΔL6MW241F double mutant that resembles some features of cyanobacterial PsbO, significantly repairs the defects in W241F. Our data suggest that the C-terminal F → W mutation likely evolved in higher plants and green algae in order to preserve proper PsbO folding and PSII binding and assembly, which promotes efficient Cl^- retention in the oxygen-evolving complex.

1. Introduction

The photosystem II (PSII) manganese-stabilizing protein (PsbO) is found in all oxygenic organisms examined thus far. The largest extrinsic polypeptide attached to the intrinsic subunits of PSII, it functions along with the other extrinsic proteins to shield the oxygen-evolving complex (OEC) active site (containing 4Mn, 1 Ca^{2+}, 1 Cl^-) from reducing agents [1], and is required for high rates of water oxidation [2]. In solution, PsbO behaves as a natively unfolded polypeptide [3,4] in which the N- and C-termini reside in proximity to one another [5], and the PsbO C-terminus resides in a hydrophobic environment [3]. A significant fraction (~56–60%) of PsbO secondary structure in solution consists of turns and random coils [6–8]. Upon assembly into PSII, PsbO retains the hydrophobic C-terminus [9–11], but the protein also undergoes additional folding by which it gains β-sheet elements at the expense of unordered structures [12]. This is consistent with the finding of Loll et al. in [9] who predicted, according to PDB entry 1S5L [10], that PSII-associated PsbO from *Thermosynechococcus elongatus* contains 44% of β-sheet, 8% of α-helix, and only 48% of unordered coils and turns. Photosystem II-bound PsbO in eukaryotes occupies two specific binding sites per PSII reaction center [2,13–15], which is consistent with the fact that binding of wild type (WT) PsbO saturates at 2 mol of PsbO per mol PSII, and remains fully saturated at higher concentrations of the protein added into reconstitution mixtures [7,8].

A number of PsbO mutants have been generated that produce an assortment of effects on the structure and/or function of the prokaryotic or eukaryotic proteins (see [16,17]). The W → F mutation in the lone Trp241 of spinach PsbO, which is conserved in PsbO from higher plants and green algae (see Table 1 and Appendix A: Supplementary data) results in detrimental effects on PSII binding and activity of the protein, and modifies its near-UV circular dichroism (CD), UV absorption, and fluorescence properties. Activity and PSII binding of W241F can be restored to near-WT levels by removal of six residues from its N-terminus, which produces the ΔL6MW241F double mutant [8]. The analogous N-terminal deletion by six residues in recombinant WT PsbO produces the ΔL6M mutated protein that exhibits WT levels of PSII binding and activity, but this protein also binds non-specifically [13]. The near-UV CD spectra of both WT PsbO and ΔL6M PsbO are very similar, and exhibit the distinct peaks that arise from aromatic amino acid residues (Trp, Tyr, Phe) buried in a hydrophobic environment

Abbreviations: BSA, bovine serum albumin; CD, circular dichroism; DCBQ, 2,6-dichloro-1,4-benzoquinone; IPTG, isopropyl-β-Δ-thiogalactopyranoside; MES, 2-(*N*-morpholino)ethanesulfonic acid; PsbO, manganese-stabilizing protein; OEC, oxygen-evolving complex; PS, photosystem; SW-PSII, NaCl-washed photosystem II membranes depleted of 23 and 17 kDa extrinsic proteins; Tris, tris(hydroxymethyl)-aminomethane; UW-PSII, urea NaCl-washed photosystem II membranes depleted of PsbO, PsbP and PsbQ (33, 23, and 17 kDa) extrinsic proteins; WT, wild type

* Corresponding author. Fax: +1 734 647 0884.
E-mail address: popelka@umich.edu (H. Popelkova).

0014-5793/$36.00
doi:10.1016/j.febslet.2010.08.011

Table 1
Amino acid sequence alignment of the N- and C-terminal domains of PsbOs.

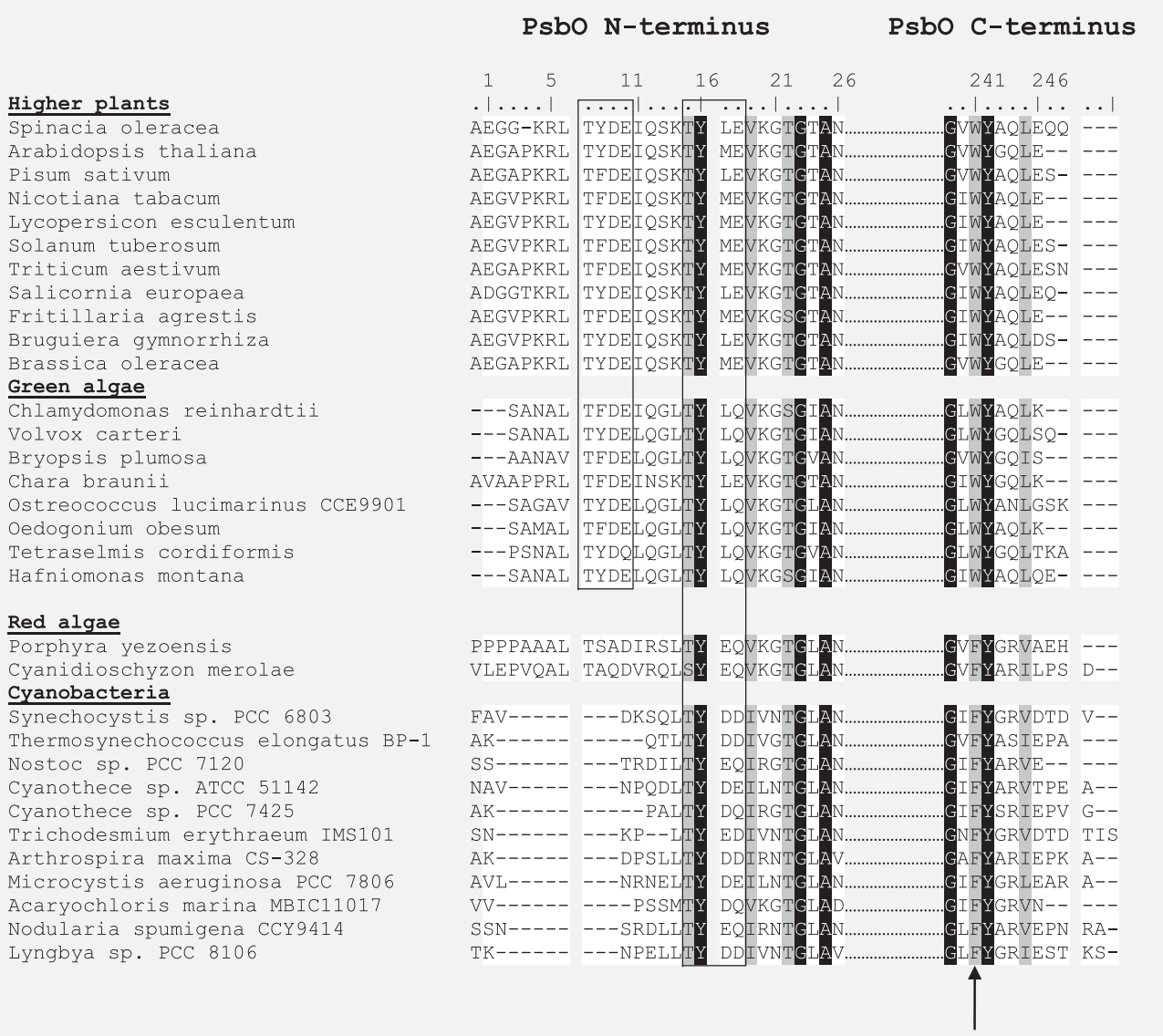

Black boxes in the N-terminal domain of PsbO highlight one or two PSII binding sequences, and the black arrow in the PsbO C-terminal domain marks the conserved Trp in higher plants and green algae and the conserved Phe at the homologous position in red algae and cyanobacteria. Black lanes mark identical amino acid residues, and grey lanes highlight similar residues. The numbers above the ruler show the positions of residues in the mature PsbO protein from spinach (*Spinacia oleracea*); N-terminal deletion by six residues, in the ΔL6M and ΔL6MW241F mutants described in this study, replaces the EGGKRL sequence with the Met residue.

[3,13]. The W241F mutation modifies the near-UV CD spectrum of PsbO, while the N-terminal truncation combined with the W241→F mutation eliminates the near-UV CD signals from Tyr and Trp, and leaves only traces of the Phe signal. While W241F PsbO is temperature-insensitive, the ΔL6MW241F double mutant is partially cold-sensitive; it reconstitutes higher activity at 22 °C than at 4 °C [8].

Here we show that inefficient retention of Cl^- in PsbO-depleted PSII membranes reconstituted with spinach W241F PsbO can be significantly rescued by reconstitution of these PSII membranes with the PsbO double mutant ΔL6MW241F, which partially resembles red algal and cyanobacterial PsbO. The double mutant, in contrast to W241F, exhibits a behavior in solution that is similar to that of spinach recombinant WT and that likely leads to proper folding and assembly of PsbO into PSII. Amino acid sequence alignment of PsbO from various organisms reveals that the only Trp residue in PsbO is conserved in higher plants and green algae and that its presence at the PsbO C-terminus coincides with the presence of two PSII binding domains (see [14]) at the protein's N-terminus. In contrast, Phe in place of Trp at the homologous position is conserved in PsbOs from red algae and cyanobacteria that have only one PSII binding domain at the protein's N-terminus. The data we present here suggest that the C-terminal F → W replacement likely evolved in PsbO from higher plants and green algae along with an extended N-terminus in order to preserve protein's ability to properly fold and assemble into PSII and to efficiently retain Cl^- in the OEC.

2. Materials and methods

2.1. Overexpression and purification of recombinant PsbO

Recombinant WT PsbO was overexpressed in *Escherichia coli*; 50 μg/ml of ampicillin was added to the LB medium and 25 μM isopropyl-β-Δ-thiogalactopyranoside was used to induce overexpression at 37 °C. Inclusion bodies were isolated as described in Ref. [18] except that the lysate pellet was resuspended in 10 mM NaCl, 20 mM bis[2-hydroxyethyl]imino-tris[hydroxymethyl]methane, (pH 6.4) to one lysate volume (the volume of lysed cells after DNAse addition), and then incubated on ice with 0.2% dodecyl-β-D-maltoside for 1 h. The WT protein was extracted from inclusion bodies by overnight incubation in solubilization buffer (3 M urea, 5% betaine (w/v), 20 mM bis–Tris (pH 6.4), and 5 mM NaCl) at 4 °C. The solubilized protein was loaded onto a Resource Q column equilibrated with solubilization buffer. Application of a linear gradient of 5–250 mM NaCl eluted the WT PsbO protein at ~150 mM NaCl. Urea was removed by dialysis of the protein in a buffer containing 100 mM Tris (pH 8) and 10 mM NaCl, and the pH was next adjusted by dialysis against 50 mM 2-(*N*-morpholino)ethanesulfonic acid (MES) (pH 6) and 10 mM NaCl. The ΔL6M, W241F, and ΔL6MW241F PsbO mutants were prepared similarly, as described in Refs. [8,13]. All recombinant proteins were stored in the SMN buffer [0.4 M sucrose, 10 mM NaCl, nd 50 mM MES (pH 6)] at −70 °C.

2.2. Reconstitution of urea NaCl-washed photosystem II membranes depleted of PsbO, PsbP and PsbQ (33, 23, and 17 kDa) extrinsic proteins (UW-PSII) with recombinant PsbO and Cl^- K_M determination

Intact PSII and UW-PSII membranes from spinach were prepared as described in Ref. [7]. The PsbO-depleted PSII that was stored at −70 °C was thawed and reconstituted with recombinant PsbO (5 mol PsbO/mol PSII) for 1 h at 23 °C in a reconstitution buffer containing 37 mM MES (pH 6), 100 μg/ml bovine serum albumin (BSA), 0.3 M sucrose, 2% betaine (w/v), 10 mM Ca^{2+} and 12 mM Cl^-. Under these conditions, maximum binding of WT or mutant PsbO is ensured; stoichiometries are given in Table 2. The Chl concentration in the reconstitution mixtures was 200 μg/ml. For activity assays to determine a Cl^- K_M, the assay buffer contained 0.4 M sucrose, 50 mM MES (pH 6), 600 μM 2,6-dichloro-1,4-benzoquinone (used as the electron acceptor), 100 μg/ml BSA, 10 mM Ca^{2+} and varying concentrations of Cl^- (0–10 mM). Each assay mixture included 15 μg of Chl. Three independent measurements of O_2 evolution activity as a function of increasing Cl^- concentration were carried out for each mutant PsbO. The averaged data points generated hyperbolic saturation curves (see Ref. [15]), consistent with a single Cl^- binding site, which were used for determination of the Cl^- K_M values employing the Michaelis–Menten equation.

2.3. UV absorbance and CD spectroscopy

The UV absorption and far-UV CD spectra of the recombinant PsbO proteins that were dissolved in 10 mM KH_2PO_4 buffer (pH 6) were obtained as described in Refs. [7,8] using an OLIS modified Cary-17 instrument and an AVIV 62 DS CD spectrometer, respectively. For measurement of far-UV CD spectra instrument parameters were as follows: wavelength scan 250–178 nm; average time 2 s; temperature change 7 °C/min; deadband 1 °C. The secondary structure contents of the PsbO proteins were predicted based on two basis sets, each of which contains five proteins that are denatured. The numbers presented here are averages of results obtained from both CONTIN/LL and CDSSTR methods (see [19]).

2.4. Homology modeling

The homology models of WT PsbO and W241F PsbO from spinach in the PSII-associated conformation were constructed using the DeepView/Swiss-PDBViewer program, available on the Internet (http://spdbv.vital-it.ch/), and the SWISS-MODEL server [20–22]. The crystallographic model of PsbO from *T. elongatus* in the PSII-associated form [11] [PDB entry 3bz2] was used as a template. The amino acid sequences of spinach and cyanobacterial PsbOs were aligned in the DeepView/Swiss-PDBViewer program before the modeled (spinach) PsbO sequence was fitted onto the template (cyanobacterial) PsbO sequence. The alignment generated a gap at the N-terminus of the cyanobacterial sequence and in the middle of the spinach sequence (see [14,16]; Appendix A: Supplementary data).

2.5. Amino acid sequence alignment and phylogenetic tree

Amino acid sequence alignment was generated in the BioEdit Sequence Alignment Editor (©1997–2004 Tom Hall Isis Pharmaceuticals, Inc.; [23]) using the PsbO sequences available at the NCBI website (http://www.ncbi.nlm.nih.gov/). The sequences of precursor, instead of mature, PsbO's were aligned, because experimental evidence is not available to identify the exact signal-peptide cleavage site in PsbO's from some less-frequently studied organisms. The unrooted phylogenetic tree was created in the BioEdit Sequence Alignment Editor using the neighbor-joining method based on the amino acid sequence alignment of precursor PsbOs that is presented in Table 1-Supplementary data.

3. Results and discussion

3.1. The role of PsbO in Cl^- retention by PSII

Crystallographic structures of PSII from thermophilic cyanobacteria indicate the presence of one [11] or two [24,25] Cl^- atoms at distances of 6.5–7 Å from the MnCa cluster. Using the

crystallographic model of PsbO from the structure of Guskov et al. ([11], PDB entry 3bz2) as a template, we constructed and overlapped the homology models of spinach WT PsbO and W241F PsbO in the PSII-associated form (Fig. 1). The models in Fig. 1 predict that W241 in WT and F241 in the mutant are buried inside the β-barrel, and participate in formation of the C-terminal β-sheet. This is in agreement with a number of previous studies [3,6,8]. In accord with the assumption that the structural organization of the OEC active site in eukaryotic PSII is analogous to that in cyanobacterial PSII, the homology models also reveal that the Cl^- cofactor in the eukaryotic OEC could be up to ~42 Å distant from PsbO-W241 (or PsbO-F241) and ~10 Å distant from the closest residue in the large flexible loop of spinach PsbO, as the C-terminus and the large flexible loop occupy the spatially distant domains of the PsbO structure.

Previous studies have shown that a high concentration of Cl^- can stabilize O_2 evolution activity of UW-PSII [26,27] and that PsbO facilitates Cl^- retention by PSII [15,28]. The data on the Cl^- K_M values presented in Table 2 for various PsbO's are consistent with these studies. They show that the ΔL6M mutant has a Cl^- K_M of 1.2 mM, which is exactly the same value as that obtained for the functionally identical mutant ΔR5M that exhibits WT activity [15]. In contrast, W241F has a Cl^- K_M of 2.4 mM; a value that is very close to that obtained for PsbO-Arg151 and PsbO-Arg161 mutants [28] and higher than what was observed for PsbO-Asp157 mutants [17]. The residues R151, R161, and D157 reside in the large flexible loop of PsbO, relatively close to the site occupied by Cl^- (see Fig. 1). Mutations in these residues significantly disrupt O_2 evolution activity of PSII, which was interpreted to indicate a defect in the functional assembly of PsbO into PSII [17,28] that takes place after docking of the protein to its PSII binding sites [29]. The Cl^- K_M (1.4 mM; Table 2) obtained here for the ΔL6MW241F double mutant shows that truncation of W241F by six N-terminal residues significantly restores efficiency of Cl^- retention by PSII, indicating a major recovery of proper PsbO assembly.

The homology models of WT and W241F PsbO in Fig. 1 predict that both proteins have identical ribbon structures in the PSII-associated form, despite the fact that the W241F mutant is severely defective in Cl^- retention compared to WT (see Table 2). Moreover, homology modeling is unable to depict the effect of the N-terminal truncation in W241F, as the template lacks the first 12 N-terminal residues (probably due to the presence of free random coils in the protein). To obtain a better insight into the dynamic behavior of PsbO that cannot be gained from the static crystal structure of the enzyme and to better understand function-structure relations in existing PsbO mutants, we employed UV absorption and CD spectroscopies to examine structural characteristics of PsbO's in solution (Fig. 2, Table 3).

Table 2
Cl^- K_M values, O_2 evolution activity, and PsbO binding affinity to PSII for SW-PSII and for UW-PSII membranes reconstituted with various spinach recombinant PsbO.

Protein	Cl^- K_M (mM)[a]	V_{max} (%)	mol of PsbO bound/mol PSII[b]
SW-PSII	0.9[c]	100	2[d]
UW-PSII + WT PsbO	1.0[c]	70[d]	2[d]
UW-PSII + ΔL6M PsbO	1.2	65[d]	2[d]
UW-PSII + ΔL6MW241F PsbO	1.4	60[e]	2[e]
UW-PSII + W241F PsbO	2.4	30[e]	0.6[e]

[a] K_M values were determined as described in [15] from oxygen-evolution activity assayed as a function of the Cl^- concentration in the assay buffer.
[b] PsbO binding to specific PSII sites when 5 mol of PsbO/mol PSII was added to the reconstitution mixture.
[c] Data from [15].
[d] Data from [13].
[e] Data from [8]; 100% V_{max} corresponds to activity of control, SW-PSII sample (250–400 μmol O_2/mg Chl/h) that contains natively bound PsbO.

3.2. Elucidation of PsbO dynamics in solution

Fig. 2 shows UV absorption spectra of PsbO's in 10 mM KH_2PO_4 (pH 6) buffer. As compared to WT, W241F exhibits a broader blue-shifted UV spectrum with a peak at 266 nm and a missing shoulder at 293 nm, features that in WT are ascribed to UV absorption from W241 in a hydrophobic environment [3,8]. In contrast, UV absorption spectra of ΔL6M and ΔL6MW241F appear to be very similar to that of WT PsbO, except that the double mutant lacks the shoulder at 293 nm, as expected owing to the loss of Tryp241. The

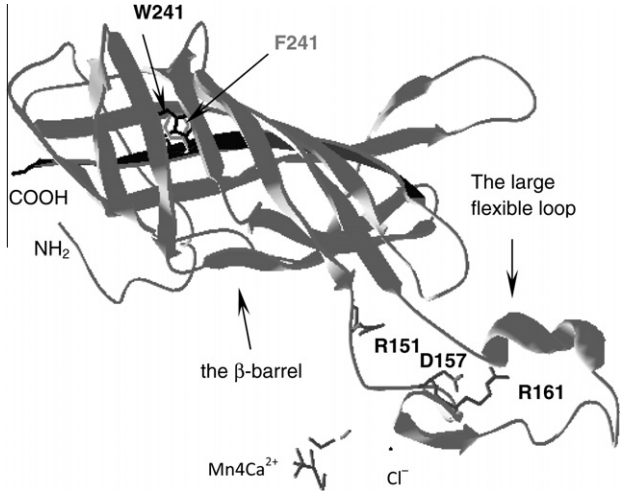

Fig. 1. Overlap of the three-dimensional homology models of WT PsbO and W241F PsbO from spinach in the PSII-associated form. A crystallographic model of PsbO from *T. elongatus* [PDB entry 3bz2] [11] was used as a template. W241 in wild type and F241 in the mutant are buried inside the β-barrel and form a part of the C-terminal β-sheet. The C-terminal β-sheet is highlighted in black; Cl^- is shown as a black dot.

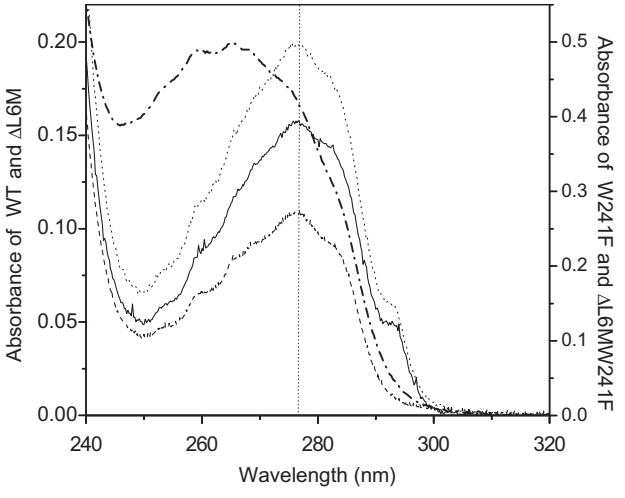

Fig. 2. UV absorption spectra of recombinant WT PsbO, W241F PsbO, ΔL6M PsbO, and ΔL6MW241F PsbO. The protein concentrations were 12 μM for WT, 52 μM for W241F, 10 μM for ΔL6M, and 34 μM for ΔL6MW241F. The proteins were dissolved in 10 mM KH_2PO_4 buffer (pH 6). Spectra are (...) for WT, (.-.-.) for W241F, (—) for ΔL6M, and (- - -) for ΔL6MW241F. The vertical dotted line indicates the 277 nm position of the UV absorption peak for WT, ΔL6M, and ΔL6MW241F. The spectra of WT and W241F are redrawn from [8] for comparison.

Table 3
Secondary structure prediction for recombinant WT PsbO, W241F PsbO, ΔL6M PsbO, and ΔL6MW241F PsbO based on analyses of far-UV CD spectra.[a]

Protein	α-Helix (%)	β-Sheet (%)	Turn + unordered (%)
WT (25 °C)[b]	4	36	60
ΔL6M (25 °C)	3	40	56
W241F (25 °C)[b]	3	38	58
ΔL6MW241F (25 °C)	3	40	56
WT (90 °C)[b]	6	25	68
ΔL6M (90 °C)	7	25 (*0*)[c]	68
W241F (90 °C)[b]	3	37 (*48*)	59
ΔL6MW241F (90 °C)	5	31 (*24*)	64
WT (25 °C cooled)[b]	3	37	59
ΔL6M (25 °C cooled)	3	38 (*3*)	59
W241F (25 °C cooled)[b]	2	42 (*14*)	53
ΔL6MW241F (25 °C cooled)	3	39 (*5*)	57

[a] The numbers are averages of results obtained from the basis sets that contain secondary structure contents from five denatures proteins. The CONTIN/LL and CDSSTR methods were used for estimation of secondary structure [19].
[b] Data from [8].
[c] Data in parenthesis represent a percent increase in the predicted β-sheet content of mutants during heating and cooling compared to WT PsbO.

observations that the ΔL6MW241F UV spectrum resembles that of WT PsbO (except for the Trp shoulder) and that the ΔL6MW241F near-UV CD spectrum lacks signals from Tyr and Trp (see [8]) would suggest that the environment of residues other than Y242 in the double mutant is similar to that in WT PsbO. Table 3 shows results characterizing the thermostability of the estimated secondary structure of all four PsbO variants; data on W241F and WT PsbO taken from Ref. [8] are shown for comparison. The CD data predict that ΔL6M loses a substantial amount of β-sheet and gains α-helix and random coil upon heating to 90 °C, and regains the original secondary structure content upon cooling to 25 °C; a behavior almost identical to that of WT PsbO. In contrast, the data in Table 3 show that W241F exhibits a behavior that is very different from that of WT. This mutant retains its β-sheet upon heating, which results in 48% higher predicted β-sheet content than is found in WT PsbO at 90 °C. Upon cooling, W241F gains even more β-sheet at the expense of α-helix and random coil, which represents an additional increase in β-sheet by ~14% compared to WT PsbO at 25 °C after cooling. This result would indicate that the heating-cooling cycle promotes formation of the β-barrel structure in W241F and therefore appears to induce protein folding in solution. Perhaps the β-sheet elements form a hydrophobic core in PsbO [6] that facilitates the protein's thermostability. In contrast, the ΔL6MW241F double mutant behaves more like the WT and ΔL6M proteins; although it exhibits additional thermostability at 90 °C compared to WT (~24% higher β-sheet), it loses ~25% of its β-sheet upon heating and regains the original secondary structure content upon cooling. These data (Fig. 2, Table 3) provide experimental evidence that W241F and ΔL6MW241F have differing solution structure flexibilities. The increased stability of the β-sheet content in W241F, which could be due to a strong interaction between the N- and C-termini [5] that was probably induced by mutation, presumably makes the PsbO structure more rigid and likely prevents the proper folding/assembly of PsbO during binding with PSII intrinsic subunits. This results in a weak binding of the protein to PSII and inefficient Cl^- retention by the OEC. Given the distance between the PsbO-W241 residue and the Cl^- site (Fig. 1), the W241F mutant may be defective in overall protein refolding that appears to be necessary for a proper assembly process. By contrast, truncation of W241F by six N-terminal residues probably functions to relax the rigid PsbO structure by weakening the N- and C-terminal interaction, and facilitates the protein folding that occurs during functional assembly of PsbO into the OEC active site [12]; as a result, the double mutant binds with a high affinity to PSII and Cl^- is retained efficiently in the OEC (Table 2).

3.3. Insight into the evolution of PsbO structure and function

The data presented here can provide some insights into the evolution of the PsbO protein. It has been reported earlier that higher plants and green algae possess two N-terminal sequences in PsbO that are required for binding of two copies of the protein to PSII, while cyanobacteria lack one N-terminal binding sequence, which can explain the presence of one PsbO subunit in prokaryotic PSII (see [14]; Table 1 and Appendix A: Supplementary data). Table 1 shows that the PsbO N-terminus from red algae possesses only one conserved N-terminal binding motif, like cyanobacterial PsbO. The table also reveals that the presence of one N-terminal binding motif in PsbO from red algae and cyanobacteria correlates with the presence of the conserved Phe at the protein's C-terminus, while the presence of two N-terminal binding motifs in PsbO from green algae and higher plants coincides with Trp in place of Phe at the homologous position. In this context, the spinach PsbO double mutant ΔL6MW241F partially resembles the red algal and cyanobacterial PsbO proteins, because it has a shorter N-terminus than spinach WT PsbO (although two N-terminal binding domains are present) and the conserved Phe in place of Trp at the homologous position at the C terminus (see Table 1 and Appendix A: Supplementary data). A PsbO double mutant lacking the N-terminal sequence of 7–14 (instead of 6) residues would possess only one intact N-terminal binding domain, like red algal and cyanobacterial PsbO (Table 1), which would likely result in binding of only one PsbO copy per PSII reaction center. We have already documented the defects arising from the lower PsbO stoichiometry in eukaryotic PSII (see [13]) that would mask the recovery of function caused by N-terminal truncation in W241F.

One of the roles of PsbO in PSII that originated over billions of years of evolution is to function as a barrier that facilitates efficient retention of Cl^- in PSII [26]. This requires that PsbO folds properly during its assembly into PSII [17,28]. Our data show that this ability is severely compromised in the W241F PsbO mutant, but not in the ΔL6MW241F PsbO double mutant, whose primary sequence resembles, in part, that of red algal and cyanobacterial PsbO (Tables 1–3, Fig. 2). The primary amino acid sequence of PsbO carries information about the evolution of the protein. Evidently, the N- and C-terminal features of cyanobacterial PsbO (i.e. one N-terminal binding domain and the FY amino acid pair at the C-terminus) were retained in red algal PsbO during evolution, which suggests that red algal PsbO is very closely related to the cyanobacterial PsbO protein, a proposal that is supported by the discovery of cyanobacterial-type PsbV and PsbU proteins in red algal PSII [30,31]. In contrast, the N- and C-termini of PsbO from green algae and higher plants likely evolved from cyanobacterial PsbO by addition of the second N-terminal binding domain; preservation of PsbO functionality (see Table 2) required a Phe → Trp replacement at the protein's C-terminus. As a result, the green algal and higher plant PsbO proteins are evolutionarily more distant from the cyanobacterial protein. This is consistent with both the phylogenetic tree of PsbO, which was generated based on the alignment of the full PsbO sequence (see Appendix A: Fig. 1 and Table 1 Supplementary data), and the earlier study that analyzed peptide fragments generated by α-chymotrypsin and *Staphylococcus aureus* V8 protease to compare solution conformation and protease digestion accessibility of PsbO from cyanobacteria, red algae, green algae and higher plants [32]. The phylogenetic tree of PsbO (Appendix A: Fig. 1) reveals that PsbO's from higher plants are separated into several branches that are evolutionarily most distant from cyanobacterial PsbO, and that PsbO's from green algae are mapped closer to the prokaryotic protein. However, the subgroup of green algal

PsbO's segregates from the subgroup of red algal and cyanobacterial PsbO's. The fact that red algal PsbO's map most closely to cyanobacterial PsbO's reflects their similarity and close evolutionary relationship. The protease study [32] showed that the cleavage patterns of cyanobacterial and red algal PsbO's are very similar to one another, but they differ from the cleavage pattern of PsbO from higher plants. The cleavage pattern of green algal PsbO involves both cyanobacterial and higher plant PsbO's [32], indicating that red algal PsbO is more closely related to the prokaryotic protein than green algal PsbO. The evolutionary relationships that are embedded in the primary (Appendix A) and tertiary [32] structure of PsbO are also embedded in the structure/arrangement of PSII. The results of a study on the presence and organization of PSII extrinsic proteins from various species were interpreted to indicate the existence of the cyanobacterial-type, red algal-type and green algal-type evolutionary lineages; the green algal-type lineage gave rise to higher plants [33,34].

4. Conclusion

The data presented here and in Ref. [8] are consistent with the conclusion that the presence of a Phe residue instead of Trp at the C-terminus of PsbO from higher plants and green algae is functionally unfavorable and thus, evolutionarily unsustainable. The C-terminal Phe → Trp alteration likely evolved in PsbO that possesses two N-terminal PSII binding sequences in order to preserve the protein's flexibility, which is required for its proper overall folding and assembly into PSII and for efficient Cl^- retention by the OEC.

Acknowledgement

This research was supported by a grant to H.P. and C.F.Y. from the National Science Foundation (MCB-0716541).

Appendix A. Supplementary data

Supplementary data associated with this article can be found, in the online version, at doi:10.1016/j.febslet.2010.08.011.

References

[1] Ghanotakis, D.F., Topper, J.N. and Yocum, C.F. (1984) Structural organization of the oxidizing side of photosystem II. Exogenous reductants reduce and destroy the Mn-complex in photosystem II membranes depleted of the 17 and 23 kDa polypeptides. Biochim. Biophys. Acta 767, 524–531.
[2] Nelson, N. and Yocum, C.F. (2006) Structure and function of photosystems I and II. Annu. Rev. Plant Biol. 57, 521–565.
[3] Lydakis-Simantiris, N., Hutchison, R.S., Betts, S.D., Barry, B.A. and Yocum, C.F. (1999) Manganese stabilizing protein of photosystem II is a thermostable, natively unfolded polypeptide. Biochemistry 38, 404–414.
[4] Uversky, V.N. (2002) What does it mean to be natively unfolded? Eur. J. Biochem. 269, 2–12.
[5] Enami, I., Kamo, M., Ohta, H., Takahashi, S., Miura, T., Kusayanagi, M., Tanabe, S., Kamei, A., Motoki, A., Hirano, M., Tomo, T. and Satoh, K. (1998) Intramolecular cross-linking of the extrinsic 33-kDa protein leads to loss of oxygen evolution but not its ability of binding to photosystem II and stabilization of the manganese cluster. J. Biol. Chem. 273, 4629–4634.
[6] Shutova, T., Irrgang, K.D., Shubin, V., Klimov, V.V. and Renger, G. (1997) Analysis of pH-induced structural changes of the isolated extrinsic 33 kiloDalton protein of photosystem II. Biochemistry 36, 6350–6358.
[7] Popelkova, H., Im, M.M., D'Auria, J., Betts, S.D., Lydakis-Simantiris, N. and Yocum, C.F. (2002) N-terminus of the photosystem II manganese stabilizing protein: effects of sequence elongation and truncation. Biochemistry 41, 2702–2711.
[8] Wyman, A.J., Popelkova, H. and Yocum, C.F. (2008) Site-directed mutagenesis of conserved C-terminal tyrosine and tryptophan residues of PsbO, the Photosystem II manganese-stabilizing protein, alters its activity and fluorescence properties. Biochemistry 47, 6490–6498.
[9] Loll, B., Gerold, G., Slowik, D., Voelter, W., Jung, C., Saenger, W. and Irrgang, K.-D. (2005) Thermostability and Ca^{2+} binding properties of wild type and heterologously expressed PsbO protein from cyanobacterial Photosystem II. Biochemistry 44, 4691–4698.
[10] Ferreira, K.N., Iverson, T.M., Maghlaoui, K., Barber, J. and Iwata, S. (2004) Architecture of the photosynthetic oxygen-evolving center. Science 303, 1831–1838.
[11] Guskov, A., Kern, J., Gabdulkhakov, A., Broser, M., Zouni, A. and Saenger, W. (2009) Cyanobacterial photosystem II at 2.9 Å resolution and the role of quinones, lipids, channels, and chloride. Nat. Struct. Mol. Biol. 16, 334–342.
[12] Hutchison, R.S., Betts, S.D., Yocum, C.F. and Barry, B.A. (1998) Conformational changes in the extrinsic manganese stabilizing protein can occur upon binding to the photosystem II reaction center: an isotope editing and FT-IR study. Biochemistry 37, 5643–5653.
[13] Popelkova, H., Im, M.M. and Yocum, C.F. (2003) Binding of manganese stabilizing protein to photosystem II: identification of essential N-terminal threonine residues and domains that prevent nonspecific binding. Biochemistry 42, 6193–6200.
[14] Popelkova, H., Im, M.M. and Yocum, C.F. (2002) N-terminal truncations of manganese stabilizing protein identify two amino acid sequences required for binding of the eukaryotic protein to photosystem II and reveal the absence of one binding-related sequence in cyanobacteria. Biochemistry 41, 10038–10045.
[15] Popelkova, H., Commet, A., Kuntzleman, T. and Yocum, C.F. (2008) Inorganic cofactor stabilization and retention: the unique functions of the two PsbO subunits of eukaryotic Photosystem II. Biochemistry 47, 12593–12600.
[16] Motoki, A., Usui, M., Shimazu, T., Hirano, M. and Katoh, S. (2002) A domain of the manganese-stabilizing protein from *Synechococcus elongatus* involved in functional binding to Photosystem II. J. Biol. Chem. 277, 14747–14756.
[17] Popelkova, H., Commet, A. and Yocum, C.F. (2009) Asp157 is required for the function of PsbO, the Photosystem II manganese-stabilizing protein. Biochemistry 48, 11920–11928.
[18] Betts, S.D., Hachigian, T.M., Pichersky, E. and Yocum, C.F. (1994) Reconstitution of the spinach oxygen-evolving complex with recombinant *Arabidopsis* manganese-stabilizing protein. Plant Mol. Biol. 26, 117–130.
[19] Sreerama, N. and Woody, R.W. (2000) Estimation of protein secondary structure from circular dichroism spectra: comparison of CONTIN, SELCON and CDSSTR methods with an expanded reference set. Anal. Biochem. 287, 252–260.
[20] Guex, N. and Peitsch, M.C. (1997) SWISS-MODEL and the Swiss-PdbViewer: an environment for comparative protein modeling. Electrophoresis 18, 2714–2723.
[21] Schwede, T., Kopp, J., Guex, N. and Peitsch, M.C. (2003) SWISS-MODEL: and automated protein homology-modeling server. Nucleic Acids Res. 31, 3381–3385.
[22] Arnold, K., Bordoli, L., Kopp, J. and Schwede, T. (2006) The SWISS-MODEL Workspace: a web-based environment for protein structure homology modeling. Bioinformatics 22, 195–201.
[23] Hall, T.A. (1999) BioEdit: a user-friendly biological sequence alignment editor and analysis program for Windows 95/98/NT. Nucleic Acids Symp. Ser. 41, 95–98.
[24] Murray, J.W., Maghlaoui, K., Kargul, J., Ishida, N., Lai, T.L., Rutherford, A.W., Sugiura, M., Boussac, A. and Barber, J. (2008) X-ray crystallography identifies two chloride binding sites in the oxygen evolving centre of Photosystem II. Energy Environ. Sci. 1, 161–166.
[25] Kawakami, K., Umena, Y., Kamyia, N. and Shen, J.-R. (2009) Location of chloride and its possible functions in oxygen-evolving photosystem II revealed by X-ray crystallography. Proc. Nat. Acad. Sci. 106, 8567–8572.
[26] Miyao, M. and Murata, N. (1984) Role of the 33 kDa polypeptide in preserving Mn in the photosynthetic oxygen-evolution system and its replacement by chloride ions. FEBS Lett. 170, 350–354.
[27] Miyao, M. and Murata, N. (1985) The Cl^- effect on photosynthetic oxygen evolution: interaction of Cl^- with 18-kDa, 24-kDa, and 33-kDa proteins. FEBS Lett. 180, 303–308.
[28] Popelkova, H., Betts, S.D., Lydakis-Simantiris, N., Im, M.M., Swenson, E. and Yocum, C.F. (2006) Mutagenesis of basic residues R151 and R161 in manganese-stabilizing protein of photosystem II causes inefficient binding of chloride to the oxygen evolving complex. Biochemistry 45, 3107–3115.
[29] Lydakis-Simantiris, N., Betts, S.D. and Yocum, C.F. (1999) Leucine 245 is a critical residue for folding and function of the manganese stabilizing protein of photosystem II. Biochemistry 38, 15528–15535.
[30] Enami, I., Murayama, H., Ohta, H., Kamo, M., Nakazato, K. and Shen, J.-R. (1995) Isolation and characterization of a Photosystem II complex from the red alga *Cyanidium caldarium*: association of cytochrome c-550 and a 12 kDa protein with the complex. Biochim. Biophys. Acta 1232, 208–216.
[31] Enami, I., Kikuchi, S., Fukuda, T., Ohta, H. and Shen, J.-R. (1998) Binding and functional properties of four extrinsic proteins of Photosystem II from a red alga *Cyanidium caldarium*, as studied by release-reconstitution experiments. Biochemistry 37, 2787–2793.
[32] Tohri, A., Suzuki, T., Okuyama, S., Kamino, K., Motoki, A., Hirano, M., Ohta, H., Shen, J.-R., Yamamoto, Y. and Enami, I. (2002) Comparison of the structure of the extrinsic 33 kDa protein from different organisms. Plant Cell Physiol. 43, 429–439.
[33] Enami, I., Suzuki, T., Tada, O., Nakada, Y., Nakamura, K., Tohri, A., Ohta, H., Inoue, I. and Shen, J.-R. (2005) Distribution of the extrinsic proteins as a potential marker for the evolution of photosynthetic oxygen-evolving photosystem II. FEBS J. 272, 5020–5030.
[34] Enami, I., Okumura, A., Nagao, R., Suzuki, T., Iwai, M. and Shen, J.-R. (2008) Structures and functions of the extrinsic proteins of photosystem II from different species. Photosynth. Res. 98, 349–363.